
Activate or Not: Learning Customized Activation

Ningning Ma¹, Xiangyu Zhang², and Jian Sun²

¹Hong Kong University of Science and Technology

²MEGVII Technology

nmaac@cse.ust.hk, {zhangxiangyu, sunjian}@megvii.com

Abstract

Modern activation layers use non-linear functions to activate the neurons. In this paper, we present a simple but effective activation function we term ACON which learns to activate the neurons or not. Surprisingly, we find Swish, the recent popular NAS-searched activation, can be interpreted as a smooth approximation to ReLU. Intuitively, in the same way, we approximate the variants in the ReLU family to the Swish family, we call ACON , which makes Swish a special case of ACON and remarkably improves the performance. Next, we present meta-ACON , which *explicitly* learns to optimize the parameter switching between non-linear (activate) and linear (inactivate) and provides a new design space. By simply changing the activation function, we improve the ImageNet top-1 accuracy rate by 6.7% and 1.8% on MobileNet-0.25 and ResNet-152, respectively.

1 Introduction

The Rectified Linear Unit (ReLU) [12, 23, 38] has become an effective component in neural networks and a foundation of many state-of-the-art computer vision algorithms. Through a sequence of advances, the Swish activation [40] searched by the Neural Architecture Search (NAS) technique achieves top accuracy on the challenging ImageNet benchmark [9, 41]. It has been shown by many practices to ease optimization and achieve better performance [17, 48]. Our goal is to interpret the mechanism behind this searched result and present more effective activation functions.

Despite the success of NAS on modern activations, a natural question to ask is: *how does the NAS-searched Swish actually work?* We show that Swish can be surprisingly represented as a smooth approximation to ReLU, by a simple and general *approximation formula* (Equ. 2).

Our method, called ACON , follows the spirit of the ReLU-Swish conversion and converts the ReLU family to ACON family by the general *approximation formula*. We show the converted functions (ACON-A , ACON-B , ACON-C) are smooth and differentiable, where Swish is merely a case of them (ACON-A). ACON is conceptually simple and does not add any computational overhead, however, it improves accuracy remarkably. To achieve this result, we identify the fixed upper/lower bounds in the gradient as the main obstacle impeding from improving accuracy and present the ACON with learnable upper/lower bounds.

Intuitively, ACON is an extension of the ReLU-Swish conversion, learning to switch between activating or not by optimizing the switching factor. However, evidence has shown that optimizing the parameter directly cannot learn to switch between linear and non-linear well. Therefore, we optimize the switching factor *explicitly* for fast learning and present meta-ACON that learns to learn whether to activate or not (see Fig. 1). Despite it seems a minor change, meta-ACON has a large impact: it improves the accuracy on various structures (even the highly-optimized and extremely deep SENet-154) and provides a new architecture design space in the meta learner, which could be layer-wise,

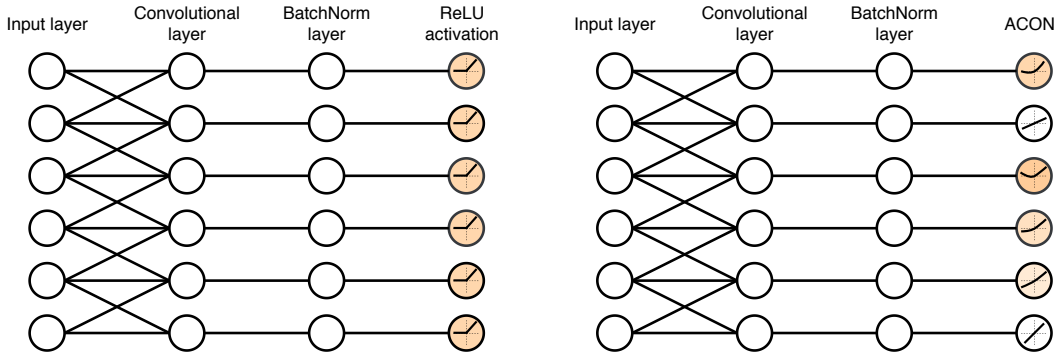


Figure 1: We present `ACON` that learns to adaptively activate the neurons or not. **Left:** ReLU network; **Right:** `ACON` network that learns to activate (orange) or not (white).

channel-wise, or pixel-wise. The design in the provided space is beyond the focus of this paper, but it is suggestive for future research.

We summarize our contributions as follows: (1) We find the NAS-searched Swish can be interestingly interpreted as a smooth approximation to ReLU; (2) In the same way, we approximate the ReLU family to be smooth and present `ACON` family as simple but effective activations; (3) We present `meta-ACON` that explicitly learns to activate the neurons or not, improves the performance remarkably, and enables a new architecture design space.

To demonstrate the effectiveness of `ACON`, we show by experiments on the challenging ImageNet [9, 41] task that `ACON` has significant improvement: it improves the ImageNet top-1 accuracy rate by 6.7% and 1.8% on MobileNet-0.25 and ResNet-152, respectively. The uncertainty of the activating degree in each layer also acts as a regularizer that can benefit generalization, and we demonstrate the generalization on object detection and semantic segmentation tasks.

2 Related Work

Activation layer The Rectified Linear Unit (ReLU) [12, 23, 38] and its variants [36, 14, 7, 34] are the most widely used activation functions in the past few years. ReLU is non-differentiable at zero and is differentiable anywhere else. Many advances followed [26, 44, 1, 16, 39, 11, 54], and softplus [10] is a smooth approximation to the maximum function ReLU based on the LogSumExp function.

The recent searching technique contributes to a new searched scalar activation called Swish [40] by combing a comprehensive set of unary functions and binary functions. The form is $y = x \cdot Sigmoid(\beta x)$, outperforms other scalar activations on some structures and datasets, and many searched results show great potential. However, there is a lack of proper explanation of Swish. In this paper, we generalize Swish to the `ACON` family, showing that it is a smooth version of ReLU based on the well-known smooth conversion called α -softmax, which is frequently applied in optimization and neural computation [27, 3, 13].

Dynamic network Standard convolution networks [43, 15, 46, 58, 6, 18, 42, 17] share the same network structure and convolution kernels for all the samples, while conditional (or dynamic) CNNs [28, 31, 53, 57, 25, 33] use dynamic kernels, widths, or depths conditioned on the input samples, obtaining remarkably gains in accuracy.

Some dynamic networks learn the dynamic kernels [55, 33], some use attention-based approaches [49, 32, 2, 50, 52, 19] to change the network structures, another series of work [51, 20] focus on dynamic depths of the convolutional networks, that skip some layers for different samples. In our work, we learn the non-linear degree in the activation function dynamically, which controls to what degree the non-linear layer is.

Neural network design space The design of the neural network architecture mainly includes the kernel level space and the feature level space. The most common feature design space aims to optimize the performance via channel dimension [46, 47, 42, 35, 19], spatial dimension [48, 4, 22]

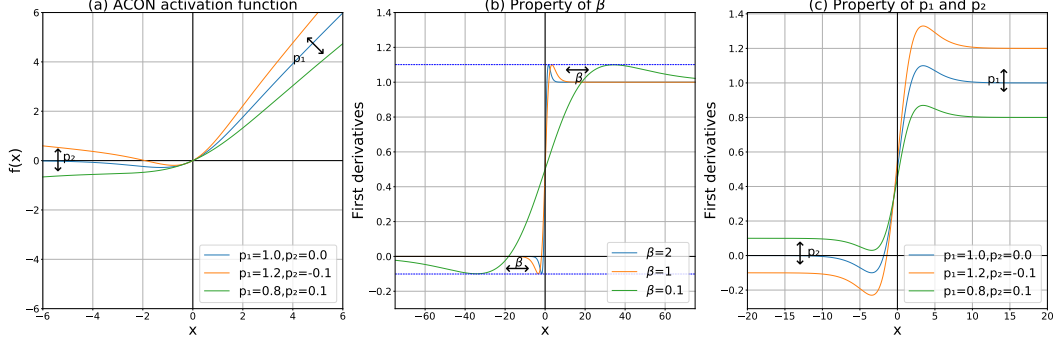


Figure 2: The ACON activation function and its first derivatives. (a) The ACON-C activation function with fixed β (see Fig. 3 for the influence of β); (b-c) The first derivatives with fixed $p_1 \& p_2$ (b) and fixed β (c). β controls how fast the first derivative asymptotes to the upper/lower bounds, which are determined by p_1 and p_2 .

and feature combination [15, 21]. On the recent popular kernel design space we can optimize the kernel shape [45, 56, 24] and kernel computation [55, 33]. In this work, we provide a new design space on the non-linear degree level by customizing the non-linear degree in each layer.

3 ACON

We present **ActivateOrNot** (ACON) as a way of learning to activate the neurons or not. In this paper, we first show how we use the general approximation formula: *smooth maximum* [27, 3, 13] to perform the ReLU-Swish [40] conversion. Next, we convert other cases in the ReLU family, which is thus a natural and intuitive idea and makes Swish a case of ACON. At last, ACON learns to activate (non-linear) or not (linear) by simply maintaining a switching factor, we introduce *meta-ACON* that learns to optimize the factor explicitly and shows significant improvements.

Smooth maximum We begin by briefly reviewing the smooth maximum function. Consider a standard maximum function $\max(x_1, \dots, x_n)$ of n values, we have its smooth and differentiable approximation:

$$S_\beta(x_1, \dots, x_n) = \frac{\sum_{i=1}^n x_i e^{\beta x_i}}{\sum_{i=1}^n e^{\beta x_i}} \quad (1)$$

where β is the switching factor: when $\beta \rightarrow \infty$, $S_\beta \rightarrow \max$; when $\beta \rightarrow 0$, $S_\beta \rightarrow$ arithmetic mean.

In neural networks, many common activation functions are in the form of $\max(\eta_a(x), \eta_b(x))$ function (e.g. ReLU $\max(x, 0)$ and its variants) where $\eta_a(x)$ and $\eta_b(x)$ denote linear functions. Our goal is to approximate the activation functions by this formula. Therefore we consider the case when $n = 2$, we denote σ as the Sigmoid function and the approximation becomes:

$$\begin{aligned} S_\beta(\eta_a(x), \eta_b(x)) &= \eta_a(x) \cdot \frac{e^{\beta \eta_a(x)}}{e^{\beta \eta_a(x)} + e^{\beta \eta_b(x)}} + \eta_b(x) \cdot \frac{e^{\beta \eta_b(x)}}{e^{\beta \eta_a(x)} + e^{\beta \eta_b(x)}} \\ &= \eta_a(x) \cdot \frac{1}{1 + e^{-\beta(\eta_a(x) - \eta_b(x))}} + \eta_b(x) \cdot \frac{1}{1 + e^{-\beta(\eta_b(x) - \eta_a(x))}} \\ &= \eta_a(x) \cdot \sigma[\beta(\eta_a(x) - \eta_b(x))] + \eta_b(x) \cdot \sigma[\beta(\eta_b(x) - \eta_a(x))] \\ &= (\eta_a(x) - \eta_b(x)) \cdot \sigma[\beta(\eta_a(x) - \eta_b(x))] + \eta_b(x) \end{aligned} \quad (2)$$

ACON-A We consider the case of ReLU when $\eta_a(x) = x, \eta_b(x) = 0$, then $f_{\text{ACON-A}}(x) = S_\beta(x, 0) = x \cdot \sigma(\beta x)$, which we call ACON-A and is exactly the formulation of Swish [40]. Swish is a recent new activation which is a NAS-searched result, although it is widely used recently, there is a lack of reasonable explanations about why it improves the performance. From the perspective above, we observe that Swish is a smooth approximation to ReLU.

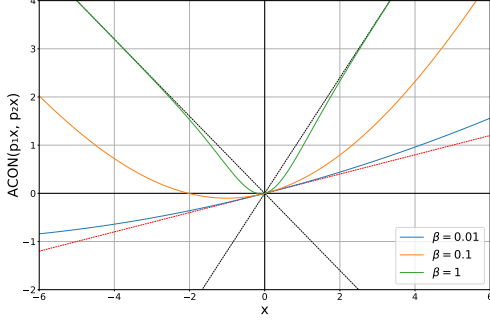


Figure 3: ACON-C applied on ‘ $1.2x$ ’ and ‘ $-0.8x$ ’ functions with various values of β , which switches between non-linear and linear (arithmetic mean). Very large β can approximate the *maximum* function (non-linear) and β near zero can approximate the *mean* function (linear) (the red dashed line).

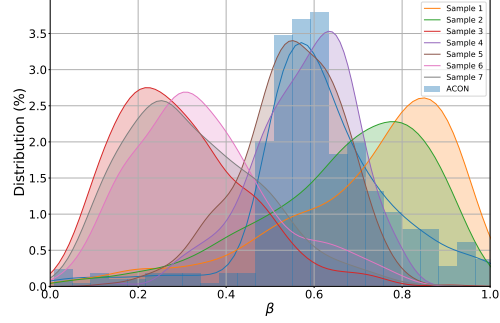


Figure 4: ACON v.s. meta-ACON. β -distribution of an activation layer in the last bottleneck of the trained ResNet-50 models. We randomly select 7 samples, for the ACON network, they share the same β distribution (the blue histogram); while for the meta-ACON network, they have 7 distinct β distributions. Lower β value means more linear, larger β value means more non-linear.

ACON-B Intuitively, based on the approximation we could convert other maximum-based activations in the ReLU family (e.g. Leaky ReLU [36], PReLU [14], etc) to the ACON family. Next, we show the approximation of PReLU. It has an original form $f(x) = \max(x, 0) + p \cdot \min(x, 0)$, where p is a learnable parameter and initialized as 0.25. However, in most case $p < 1$, under this assumption, we rewrite it to the form: $f(x) = \max(x, px)$ ($p < 1$). Therefore we consider the case when $\eta_a(x) = x$, $\eta_b(x) = px$ in Equ. 2 and get the following new activation we call ACON-B:

$$f_{\text{ACON-B}}(x) = S_{\beta}(x, px) = (1 - p)x \cdot \sigma[\beta(1 - p)x] + px \quad (3)$$

ACON-C Intuitively, we present a simple and more general case we term ACON-C. We adopt the same two-argument function, with an additional hyper-parameter. ACON-C follows the spirit of ACON-B that simply uses hyper-parameters scaling on the feature. Formally, let $\eta_a(x) = p_1x$, $\eta_b(x) = p_2x$ ($p_1 \neq p_2$):

$$f_{\text{ACON-C}}(x) = S_{\beta}(p_1x, p_2x) = (p_1 - p_2)x \cdot \sigma[\beta(p_1 - p_2)x] + p_2x \quad (4)$$

Our definition of ACON-C is a very simple and general case (see Fig. 2, Fig. 3). Moreover, there could be many more complicated cases in the ReLU family (e.g. more complicated formulations of $\eta_a(x)$ and $\eta_b(x)$), which are beyond the scope of this paper. We focus on the property of the conversion on this simple form.

Upper/lower bounds in the first derivative. We show that Swish has fixed upper/lower bounds (Fig. 2 b) but our definition of ACON-C allows the gradient has learnable upper/lower bounds (Fig. 2 c). Formally, we compute the first derivative of ACON-C and its limits as follows:

$$\frac{d}{dx}[f_{\text{ACON-C}}(x)] = \frac{(p_1 - p_2)(1 + e^{-\beta(p_1x - p_2x)}) + \beta(p_1 - p_2)^2 e^{-\beta(p_1x - p_2x)}x}{(1 + e^{-\beta(p_1x - p_2x)})^2} + p_2 \quad (5)$$

$$\lim_{x \rightarrow \infty} \frac{df_{\text{ACON-C}}(x)}{dx} = p_1, \quad \lim_{x \rightarrow -\infty} \frac{df_{\text{ACON-C}}(x)}{dx} = p_2 \quad (\beta > 0) \quad (6)$$

To compute the upper/lower bounds, which are the maxma/minima values, we compute the second derivative:

$$\frac{d^2}{dx^2}[f_{\text{ACON-C}}(x)] = \frac{\beta(p_2 - p_1)^2 e^{\beta(p_1 - p_2)x} ((\beta(p_2 - p_1)x + 2)e^{\beta(p_1 - p_2)x} + \beta(p_1 - p_2)x + 2)}{(e^{\beta(p_1 - p_2)x} + 1)^3} \quad (7)$$

We set $\frac{d^2}{dx^2}[f_{\text{ACON-C}}(x)] = 0$, simplify it, and get $(y - 2)e^y = y + 2$, where $y = (p_1 - p_2)\beta x$. Solving the equation we get $y \approx \pm 2.39936$. Then we get maxima and minima of Equ. 5:

$$\begin{aligned} \text{maxima}(\frac{d}{dx}[f_{\text{ACON-C}}(x)]) &\approx 1.0998p_1 - 0.0998p_2, \\ \text{minima}(\frac{d}{dx}[f_{\text{ACON-C}}(x)]) &\approx 1.0998p_2 - 0.0998p_1 \quad (\beta > 0) \end{aligned} \tag{8}$$

This is different from Swish with the fixed upper/lower bounds (1.0998, -0.0998) in the first derivative. In Swish, the hyper-parameter β only determines how fast the first derivative asymptotes to the upper bound and the lower bound, however, the bounds are learnable and determined by p_1 and p_2 in ACON-C (see Fig. 2 c). The learnable boundaries are essential to ease optimization and we show by experiments that these learnable upper/lower bounds are the key for improved results.

Table 1: Summary of the ReLU family and ACON family. σ denotes Sigmoid.

		ReLU family	ACON activation family
$\eta_a(x)$	$\eta_b(x)$	$\max(\eta_a(x), \eta_b(x))$	$(\eta_a(x) - \eta_b(x)) \cdot \sigma(\beta(\eta_a(x) - \eta_b(x))) + \eta_b(x)$
x	0	$\max(x, 0) : \text{ReLU}$	$\text{ACON-A}(\text{Swish}) : x \cdot \sigma(\beta x)$
x	px	$\max(x, px) : \text{PReLU}$	$\text{ACON-B} : (1 - p)x \cdot \sigma(\beta(1 - p)x) + px$
p_1x	p_2x	$\max(p_1x, p_2x)$	$\text{ACON-C} : (p_1 - p_2)x \cdot \sigma(\beta(p_1 - p_2)x) + p_2x$

3.1 Meta-ACON

ACON switches the activation to activate or not as the switching factor β controls it to be non-linear or linear. Specifically, when $\beta \rightarrow \infty$, $f_{\text{ACON-C}}(x) \rightarrow \max(p_1x, p_2x)$; when $\beta \rightarrow 0$, $f_{\text{ACON-C}}(x) \rightarrow \text{mean}(p_1x, p_2x)$. Thus, unlike the traditional activations such as the ReLU family, ACON allows each neuron to adaptively activate or not (see Fig. 1). This customized activating behavior helps to improve generalization and transfer performance. This motivated us to develop the following meta-ACON that plays a key role in the customized activation.

Our proposed concept is simple: learning the switching factor β explicitly conditioned on the input sample $x \in \mathbb{R}^{C \times H \times W}$: $\beta = G(x)$. We are not aiming to propose a specific structure, we provide a design space in the generating function $G(x)$.

Design space The concept is more important than the specific architecture which can be layer-wise, channel-wise or pixel-wise structure. Our goal is to present some simple designing examples, which manage to obtain significantly improved accuracy and show the importance of this new design space.

We briefly use a routing function to compute β conditioned on input features and present some simple structures. First, the structure can be layer-wise, which means the elements in a layer share the same switching factor. Formally, we have: $\beta = \sigma \sum_{c=1}^C \sum_{h=1}^H \sum_{w=1}^W x_{c,h,w}$.

Second, we present a simple channel-wise structure, meaning the elements in a channel share the same switching factor. Formally, we show it by: $\beta_c = \sigma W_1 W_2 \sum_{h=1}^H \sum_{w=1}^W x_{c,h,w}$. We use $W_1 \in \mathbb{R}^{C \times C/r}$, $W_2 \in \mathbb{R}^{C/r \times C}$ to save parameters ($r = 16$ by default).

Third, for the pixel-wise structure, all the elements use unique factors. Although there could be many structure designing methods, we simply present an extremely simple structure aiming to present a pixel-wise example. Formally, we have: $\beta_{c,h,w} = \sigma x_{c,h,w}$.

We note that our meta-ACON has a straightforward structure. For the following meta-ACON experiments, we use the channel-wise structure and ACON-C unless otherwise noted. More complex designs have the potential to improve performance but are not the focus of this work.

Table 2: **Comprehensive comparison of ACON on MobileNets, ShuffleNetV2 and ResNets.** We report the top-1 error on the ImageNet dataset (train and test on 224x224 input size).

Model	MobileNet		MobileNetV2		ShuffleNetV2		ResNet		
Channel / depth	0.25	0.75	0.17	1.0	0.5x	1.5x	Res-18	Res-50	Res-101
FLOPs	41M	325M	42M	300M	41M	300M	1.8G	3.9G	11.3G
ReLU	47.6	30.2	52.6	27.9	39.4	27.4	30.3	24.0	22.8
ACON-A (Swish)	44.8	28.9	51.4	27.3	38.3	26.8	30.3	23.5	22.7
ACON-B	44.0	28.7	50.8	26.4	38.0	26.8	29.4	23.3	22.3
ACON-C	43.7	28.4	48.9	26.4	37.0	26.5	29.1	23.2	22.1

Table 3: **Comparison of the meta-ACON on MobileNets, ShuffleNetV2, and ResNets.** We report the top-1 error on the ImageNet dataset (train and test on 224x224 input size).

	ReLU			meta-ACON		
	FLOPs	# Params.	Top-1 err.	FLOPs	# Params.	Top-1 err.
MobileNetV1 0.25	41M	0.5M	47.6	41M	0.6M	40.9 _(+6.7)
MobileNetV2 0.17	42M	1.4M	52.6	42M	1.9M	46.2 _(+6.4)
ShuffleNetV2 0.5x	41M	1.4M	39.4	41M	1.7M	34.8 _(+4.6)
MobileNetV1 0.75	325M	2.6M	30.2	326M	3.1M	26.4 _(+3.8)
MobileNetV2 1.0	299M	3.5M	27.9	299M	3.9M	25.0 _(+2.9)
ShuffleNetV2 1.5x	301M	3.4M	27.4	304M	6.0M	24.7 _(+2.7)
ResNet-18	1.8G	11.7M	30.3	1.8G	11.9M	28.4 _(+1.9)
ResNet-50	3.9G	25.5M	24.0	3.9G	25.7M	22.0 _(+2.0)
ResNet-101	7.3G	44.1M	22.8	7.3G	44.1M	21.1 _(+1.7)
ResNet-152	11.3G	60.0M	22.3	11.3G	60.1M	20.5 _(+1.8)

4 Experiment

4.1 Image Classification

We present a thorough experimental comparison on the challenging ImageNet 2012 classification dataset [9, 41] along with comprehensive ablations. For training, we follow the common practice and train all the models using the same input size of 224x224 and report the standard top-1 error rate.

ACON We first evaluate our ACON method on the light-weight CNNs (MobileNets [18, 42] and ShuffleNetV2 [35]) and deep CNNs (ResNets [15]). For light-weight CNNs we follow the training configure in [35]; for the larger model ResNet, we use linear decay learning rate schedule from 0.1, a weight decay of 1e-4, a batch size of 256, and 600k iterations. We run numerous experiments to analyze the behavior of the ACON activation function, by simply changing all the activations on various network structures and various model sizes. The baseline networks are the ReLU networks and the extra parameters in ACON networks are negligible.

We have two major observations from Table 2 and Fig. 2. (i), ACON-A, ACON-B, and ACON-C all improve the accuracy remarkably comparing with their *max-based* functions. This shows the benefits of the differentiable and smooth conversion. (ii), ACON-C outperforms ACON-A (Swish) and ACON-B, benefitting from the adaptive upper/lower bounds in the ACON-C’s first derivatives. (iii), Although ACON-A (Swish) shows minor improvements as the models go deeper and larger (0.1% on ResNet-101), we still obtain continuous accuracy gains from ACON-C (0.7% on ResNet-101).

Meta-ACON Next, we evaluate the meta-ACON function. For light-weight CNNs we change all the ReLU activations to meta-ACON, for deep CNN (ResNet-50, ResNet-101) we change one ReLU (after the 3×3 convolution) in each building block to meta-ACON to avoid the overfitting problem.

The results in Table 3 show that we manage to obtain remarkably accuracy gains in all the network structures. For light-weight CNNs, meta-ACON improves 6.7% on MobileNetV1 0.25 and still has

Table 4: **Comparison with other activations.** We report the top-1 error on the ImageNet dataset.

Activation	Top-1 err.
ReLU	39.4
Swish [40]	38.3
Mish [37]	39.5
ELU [7]	39.5
SoftPlus[10]	39.6
ACON-C	37.0
meta-ACON	34.8

Table 6: **Meta-ACON v.s. SENet [19].** We report the ImageNet top-1 error rates of ShuffleNetV2 and ResNet.

	Baseline	SE	meta-ACON
ShuffleNetV2 0.5x	39.4	37.5	34.8
ShuffleNetV2 1.5x	27.4	26.4	24.7
ResNet-50	24.0	22.8	22.0
ResNet-101	22.8	21.9	21.1
ResNet-152	22.3	21.5	20.5

Table 5: **Design space in meta-ACON.** We report the top-1 error on the ImageNet dataset. Comparison on 3 different levels of design space. We give 3 most simple examples on ShuffleNetV2 0.5x. fc denotes fully-connected, σ denotes sigmoid, GAP denotes global average pooling.

	manner	Top-1 err.
baseline	-	39.4
pixel-wise	$\sigma(x)$	37.2
channel-wise	$\sigma(fc[fc[GAP(x)]])$	34.8
layer-wise	$\sigma[\sum_c GAP(x)]$	36.3

Table 7: **Comparison on the extremely deep SENet-154 [19].** We report the ImageNet top-1 error rates. We implement all the models by ourselves.

Activation	Top-1 err.
ReLU	18.95
ACON-A (Swish)	19.02
ACON-C	18.40

around 3% accuracy gains on 300M level models. For deeper ResNets, meta-ACON still shows significant improvements, which are 2.0% and 1.7% on ResNet-50 and ResNet-101.

To reveal the reasons, in Fig. 4 we select a layer in the last bottleneck and compare the learned β distribution in ResNet-50. ACON shares the same β distribution for all the different samples across the dataset, however, in meta-ACON different samples have distinct non-linear degrees instead of sharing the same non-linear degree in ACON. Specifically, some samples tend to have more values close to zero, which means for such samples the network tends to have a lower non-linear degree. While some samples tend to have more values far from zero, meaning the network adaptively learns a higher non-linearity for such samples. This is an intuitively reasonable result as different samples usually have quite different characteristics and properties.

4.2 Ablation Study

We run several ablations to analyze the proposed ACON and meta-ACON activations.

Comparison with other activations Table 4 show the comparison with more activations besides ReLU and Swish, including Mish [37], ELU [7], SoftPlus [10]. We note that recent advances show comparable results comparing with ReLU, except that Swish shows greater improvement (1.1% top-1 error rate). ACON and meta-ACON manage to improve the accuracy remarkably (2.4% and 4.6%) comparing with the previous activations.

Design space in meta-ACON We provide a new architecture design space in meta-ACON ($G(x)$ in Sec. 3.1). As the switching factor determines the non-linearity in the activation, we generate β values for each sample on different levels, which could be pixel-wise, channel-wise, and layer-wise. Our goal is to present a wide design space that provides more possibilities in the future neural network design, we are not aiming to propose the most effective specific module in this paper, which is worth more future studies. We investigate the most simple module for each level that is described in Section 3.1. Table 5 shows the comparison on ShuffleNetV2 0.5x. The results show that all three levels could improve accuracy significantly, with more careful design, there could be more effective modules.

Switching factor distribution In meta-ACON we adopt a meta-learning module to learn the switching factor β explicitly. Figure 4 shows the distribution of the learned factor in the last activation layer of ResNet-50, we compare meta-ACON with ACON, and randomly select 7 samples to show the result.

Table 8: **Comparison of different activations on the COCO object detection [30] task.** We report results on RetinaNet [29] with ResNet-50 backbones.

	mAP	AP_{50}	AP_{75}	AP_S	AP_M	AP_L
ReLU	35.2	53.7	37.5	18.8	39.7	48.8
Swish	35.8	54.1	38.7	18.6	40.0	49.4
meta-ACON	36.5	55.9	38.9	19.9	40.7	50.6

Table 9: **Comparison of different activations on the CityScape [8] semantic segmentation task.** We report results on PSPNet [59] with ResNet-50 backbones.

Activation	FLOPs	# Params.	mean_IU
ReLU	3.9G	25.5M	77.2
Swish	3.9G	25.5M	77.5
meta-ACON	3.9G	25.7M	78.3

The distributions indicate three conclusions: (1) meta-ACON learns a more widespread distribution than ACON; (2) each sample has its own switching factor instead of sharing the same one; (3) some samples have more values close to zero, meaning some neurons tend not to activate in this layer.

Comparison with SENet We have shown that ACON helps improving accuracy remarkably. Next, we compare our channel-wise meta-ACON with the effective module SENet [19] on various structures. We conduct a comprehensive comparison of both light-weight CNNs and deep CNNs. Table 6 shows that meta-ACON outperforms SENet significantly on all the network structures. We note that it is more difficult to improve accuracy on larger networks because of highly optimized, but we find that even in the extreme deep ResNet-152, meta-ACON still improves accuracy by 1.8%, which gains 1% comparing with SENet.

Moreover, we conduct experiments on the highly optimized and extremely large network SENet-154 [19], which is challenging to further improve the accuracy. We re-implement SENet-154 and change the activations to ACON under the same experimental environment for fairness comparison. We note that SE together with ACON-A or ACON-C is a case of channel-wise meta-ACON structure, the differences between them are the learnable upper/lower bounds (see Sec.3). Table 7 shows two results: first, simply combing ACON-A (Swish) with SENet performs comparable or even worse result comparing to ReLU activation; second, ACON-C achieves 18.40 top-1 error rate on the challenging ImageNet dataset, improving the performance remarkably.

4.3 Generalization

Our framework can easily be extended to other tasks, we show by experiments on object detection and semantic segmentation that it has good generalization performance.

COCO object detection We report the standard COCO [30] metrics including AP (averaged over IoU thresholds), AP_{50} , AP_{75} , AP_S , AP_M , AP_L (AP at different scales). We train using the union of 80k train images and a 35k subset of validation images (*trainval35k*) and report results on the remaining 5k validation images (*minival*). We choose the RetinaNet [29] as the detector and use ResNet-50 as the backbone. As a common practice, we use a batch size of 2, a weight decay of $1e-4$, and a momentum of 0.9. We use anchors for 3 scales and 3 aspect ratios and use a 600-pixel train and test image scale. To evaluate the results of different activations, we use the ImageNet pre-trained ResNet-50 with different activations as backbones. Table 8 shows the significant improvements comparing with other activations.

Semantic segmentation We further present the semantic segmentation results on the CityScape dataset [8]. We use the PSPNet [59] as the segmentation framework and ResNet-50 as the backbone. As a common practice, we use the poly learning rate policy where the base is 0.01 and the power is 0.9, a weight decay of $1e-4$, and a batch size of 16. Table 9 shows that our result (78.3) is 1.1 points

higher than the ReLU baseline, showing larger improvement than Swish. Given the effectiveness of our method on various tasks, we expect it to be a robust and effective activation for other tasks.

5 Conclusion

In this work, we present `ACON` as a general and effective activation that learns to activate or not. We show `ACON` family that approximates to the ReLU family, exploring more functions in the ReLU family is a promising future direction yet beyond the focus of this work. Moreover, to explicitly learn the switching factor that switches between linear and non-linear, we present `meta-ACON` that also provides a wide design space. Our approach is simple but highly effective, we demonstrate its efficacy on light-weight models and even improve the accuracy remarkably on the highly optimized deep SENet-154. We expect this robust and effective activation applied to a wide range of applications.

References

- [1] Agostinelli, F., Hoffman, M., Sadowski, P., and Baldi, P. (2014). Learning activation functions to improve deep neural networks. *arXiv preprint arXiv:1412.6830*.
- [2] Bahdanau, D., Cho, K., and Bengio, Y. (2014). Neural machine translation by jointly learning to align and translate. *arXiv preprint arXiv:1409.0473*.
- [3] Boyd, S. P. and Vandenberghe, L. (2006). Convex optimization. *IEEE Transactions on Automatic Control*, 51:1859–1859.
- [4] Cao, Y., Xu, J., Lin, S., Wei, F., and Hu, H. (2019). Gcnet: Non-local networks meet squeeze-excitation networks and beyond. In *Proceedings of the IEEE International Conference on Computer Vision Workshops*, pages 0–0.
- [5] Chen, Y., Dai, X., Liu, M., Chen, D., Yuan, L., and Liu, Z. (2019). Dynamic convolution: Attention over convolution kernels. *arXiv preprint arXiv:1912.03458*.
- [6] Chollet, F. (2017). Xception: Deep learning with depthwise separable convolutions. In *Proceedings of the IEEE conference on computer vision and pattern recognition*, pages 1251–1258.
- [7] Clevert, D.-A., Unterthiner, T., and Hochreiter, S. (2015). Fast and accurate deep network learning by exponential linear units (elus). *arXiv preprint arXiv:1511.07289*.
- [8] Cordts, M., Omran, M., Ramos, S., Rehfeld, T., Enzweiler, M., Benenson, R., Franke, U., Roth, S., and Schiele, B. (2016). The cityscapes dataset for semantic urban scene understanding. In *Proceedings of the IEEE conference on computer vision and pattern recognition*, pages 3213–3223.
- [9] Deng, J., Dong, W., Socher, R., Li, L.-J., Li, K., and Fei-Fei, L. (2009). Imagenet: A large-scale hierarchical image database. In *2009 IEEE conference on computer vision and pattern recognition*, pages 248–255. Ieee.
- [10] Dugas, C., Bengio, Y., Bélisle, F., Nadeau, C., and Garcia, R. (2000). Incorporating second-order functional knowledge for better option pricing. In *NIPS*.
- [11] Elfving, S., Uchibe, E., and Doya, K. (2018). Sigmoid-weighted linear units for neural network function approximation in reinforcement learning. *Neural Networks*, 107:3–11.
- [12] Hahnloser, R. H., Sarpeshkar, R., Mahowald, M. A., Douglas, R. J., and Seung, H. S. (2000). Digital selection and analogue amplification coexist in a cortex-inspired silicon circuit. *Nature*, 405(6789):947–951.
- [13] Haykin, S. (1998). *Neural networks: A comprehensive foundation*.
- [14] He, K., Zhang, X., Ren, S., and Sun, J. (2015). Delving deep into rectifiers: Surpassing human-level performance on imagenet classification. In *Proceedings of the IEEE international conference on computer vision*, pages 1026–1034.

- [15] He, K., Zhang, X., Ren, S., and Sun, J. (2016). Deep residual learning for image recognition. In *Proceedings of the IEEE conference on computer vision and pattern recognition*, pages 770–778.
- [16] Hendrycks, D. and Gimpel, K. (2016). Bridging nonlinearities and stochastic regularizers with gaussian error linear units.
- [17] Howard, A., Sandler, M., Chu, G., Chen, L.-C., Chen, B., Tan, M., Wang, W., Zhu, Y., Pang, R., Vasudevan, V., et al. (2019). Searching for mobilenetv3. In *Proceedings of the IEEE International Conference on Computer Vision*, pages 1314–1324.
- [18] Howard, A. G., Zhu, M., Chen, B., Kalenichenko, D., Wang, W., Weyand, T., Andreetto, M., and Adam, H. (2017). Mobilenets: Efficient convolutional neural networks for mobile vision applications. *arXiv preprint arXiv:1704.04861*.
- [19] Hu, J., Shen, L., and Sun, G. (2018). Squeeze-and-excitation networks. In *Proceedings of the IEEE conference on computer vision and pattern recognition*, pages 7132–7141.
- [20] Huang, G., Chen, D., Li, T., Wu, F., van der Maaten, L., and Weinberger, K. Q. (2017). Multi-scale dense networks for resource efficient image classification. *arXiv preprint arXiv:1703.09844*.
- [21] Huang, G., Liu, Z., and Weinberger, K. Q. (2016). Densely connected convolutional networks. *2017 IEEE Conference on Computer Vision and Pattern Recognition (CVPR)*, pages 2261–2269.
- [22] Jaderberg, M., Simonyan, K., Zisserman, A., et al. (2015). Spatial transformer networks. In *Advances in neural information processing systems*, pages 2017–2025.
- [23] Jarrett, K., Kavukcuoglu, K., Ranzato, M., and LeCun, Y. (2009). What is the best multi-stage architecture for object recognition? In *2009 IEEE 12th international conference on computer vision*, pages 2146–2153. IEEE.
- [24] Jeon, Y. and Kim, J. (2017). Active convolution: Learning the shape of convolution for image classification. In *Proceedings of the IEEE Conference on Computer Vision and Pattern Recognition*, pages 4201–4209.
- [25] Keskin, C. and Izadi, S. (2018). Splinenets: continuous neural decision graphs. In *Advances in Neural Information Processing Systems*, pages 1994–2004.
- [26] Klambauer, G., Unterthiner, T., Mayr, A., and Hochreiter, S. (2017). Self-normalizing neural networks. In *Advances in neural information processing systems*, pages 971–980.
- [27] Lange, M., Zühlke, D., Holz, O., and Villmann, T. (2014). Applications of lp-norms and their smooth approximations for gradient based learning vector quantization. In *ESANN*.
- [28] Lin, J., Rao, Y., Lu, J., and Zhou, J. (2017a). Runtime neural pruning. In *Advances in Neural Information Processing Systems*, pages 2181–2191.
- [29] Lin, T.-Y., Goyal, P., Girshick, R., He, K., and Dollár, P. (2017b). Focal loss for dense object detection. In *Proceedings of the IEEE international conference on computer vision*, pages 2980–2988.
- [30] Lin, T.-Y., Maire, M., Belongie, S., Hays, J., Perona, P., Ramanan, D., Dollár, P., and Zitnick, C. L. (2014). Microsoft coco: Common objects in context. In *European conference on computer vision*, pages 740–755. Springer.
- [31] Liu, L. and Deng, J. (2018). Dynamic deep neural networks: Optimizing accuracy-efficiency trade-offs by selective execution. In *Thirty-Second AAAI Conference on Artificial Intelligence*.
- [32] Luong, M.-T., Pham, H., and Manning, C. D. (2015). Effective approaches to attention-based neural machine translation. *arXiv preprint arXiv:1508.04025*.
- [33] Ma, N., Zhang, X., Huang, J., and Sun, J. (2020a). Weightnet: Revisiting the design space of weight networks.
- [34] Ma, N., Zhang, X., and Sun, J. (2020b). Funnel activation for visual recognition.

- [35] Ma, N., Zhang, X., Zheng, H.-T., and Sun, J. (2018). Shufflenet v2: Practical guidelines for efficient cnn architecture design. In *Proceedings of the European Conference on Computer Vision (ECCV)*, pages 116–131.
- [36] Maas, A. L., Hannun, A. Y., and Ng, A. Y. (2013). Rectifier nonlinearities improve neural network acoustic models. In *Proc. icml*, volume 30, page 3.
- [37] Mishra, D. (2019). Mish: A self regularized non-monotonic neural activation function. *ArXiv*, abs/1908.08681.
- [38] Nair, V. and Hinton, G. E. (2010). Rectified linear units improve restricted boltzmann machines. In *Proceedings of the 27th international conference on machine learning (ICML-10)*, pages 807–814.
- [39] Qiu, S., Xu, X., and Cai, B. (2018). Frelu: Flexible rectified linear units for improving convolutional neural networks. In *2018 24th International Conference on Pattern Recognition (ICPR)*, pages 1223–1228. IEEE.
- [40] Ramachandran, P., Zoph, B., and Le, Q. V. (2017). Searching for activation functions. *arXiv preprint arXiv:1710.05941*.
- [41] Russakovsky, O., Deng, J., Su, H., Krause, J., Satheesh, S., Ma, S., Huang, Z., Karpathy, A., Khosla, A., Bernstein, M., et al. (2015). Imagenet large scale visual recognition challenge. *International journal of computer vision*, 115(3):211–252.
- [42] Sandler, M., Howard, A., Zhu, M., Zhmoginov, A., and Chen, L.-C. (2018). Mobilenetv2: Inverted residuals and linear bottlenecks. In *Proceedings of the IEEE conference on computer vision and pattern recognition*, pages 4510–4520.
- [43] Simonyan, K. and Zisserman, A. (2014). Very deep convolutional networks for large-scale image recognition. *arXiv preprint arXiv:1409.1556*.
- [44] Singh, S. and Krishnan, S. (2019). Filter response normalization layer: Eliminating batch dependence in the training of deep neural networks. *arXiv preprint arXiv:1911.09737*.
- [45] Szegedy, C., Ioffe, S., Vanhoucke, V., and Alemi, A. A. (2017). Inception-v4, inception-resnet and the impact of residual connections on learning. In *Thirty-first AAAI conference on artificial intelligence*.
- [46] Szegedy, C., Liu, W., Jia, Y., Sermanet, P., Reed, S., Anguelov, D., Erhan, D., Vanhoucke, V., and Rabinovich, A. (2015). Going deeper with convolutions. In *Proceedings of the IEEE conference on computer vision and pattern recognition*, pages 1–9.
- [47] Szegedy, C., Vanhoucke, V., Ioffe, S., Shlens, J., and Wojna, Z. (2016). Rethinking the inception architecture for computer vision. In *Proceedings of the IEEE conference on computer vision and pattern recognition*, pages 2818–2826.
- [48] Tan, M. and Le, Q. V. (2019). Efficientnet: Rethinking model scaling for convolutional neural networks. *arXiv preprint arXiv:1905.11946*.
- [49] Vaswani, A., Shazeer, N., Parmar, N., Uszkoreit, J., Jones, L., Gomez, A. N., Kaiser, Ł., and Polosukhin, I. (2017). Attention is all you need. In *Advances in neural information processing systems*, pages 5998–6008.
- [50] Wang, F., Jiang, M., Qian, C., Yang, S., Li, C., Zhang, H., Wang, X., and Tang, X. (2017). Residual attention network for image classification. In *Proceedings of the IEEE Conference on Computer Vision and Pattern Recognition*, pages 3156–3164.
- [51] Wang, X., Yu, F., Dou, Z.-Y., Darrell, T., and Gonzalez, J. E. (2018). Skipnet: Learning dynamic routing in convolutional networks. In *Proceedings of the European Conference on Computer Vision (ECCV)*, pages 409–424.
- [52] Woo, S., Park, J., Lee, J.-Y., and So Kweon, I. (2018). Cbam: Convolutional block attention module. In *Proceedings of the European Conference on Computer Vision (ECCV)*, pages 3–19.

- [53] Wu, Z., Nagarajan, T., Kumar, A., Rennie, S., Davis, L. S., Grauman, K., and Feris, R. (2018). Blockdrop: Dynamic inference paths in residual networks. In *Proceedings of the IEEE Conference on Computer Vision and Pattern Recognition*, pages 8817–8826.
- [54] Xu, B., Wang, N., Chen, T., and Li, M. (2015). Empirical evaluation of rectified activations in convolutional network. *arXiv preprint arXiv:1505.00853*.
- [55] Yang, B., Bender, G., Le, Q. V., and Ngiam, J. (2019). Condconv: Conditionally parameterized convolutions for efficient inference. In *Advances in Neural Information Processing Systems*, pages 1305–1316.
- [56] Yu, F. and Koltun, V. (2015). Multi-scale context aggregation by dilated convolutions. *arXiv preprint arXiv:1511.07122*.
- [57] Yu, J., Yang, L., Xu, N., Yang, J., and Huang, T. (2018). Slimmable neural networks. *arXiv preprint arXiv:1812.08928*.
- [58] Zhang, X., Zhou, X., Lin, M., and Sun, J. (2018). Shufflenet: An extremely efficient convolutional neural network for mobile devices. In *Proceedings of the IEEE conference on computer vision and pattern recognition*, pages 6848–6856.
- [59] Zhao, H., Shi, J., Qi, X., Wang, X., and Jia, J. (2017). Pyramid scene parsing network. In *Proceedings of the IEEE conference on computer vision and pattern recognition*, pages 2881–2890.